

1
2
3
4
5
6
7
8
9
10
11
12
13
14
15
16
17
18
19
20
21
22
23
24
25
26
27
28

Supplementary Information

A mechanically adaptive hydrogel neural interface based on silk fibroin for high efficiency neural activity recording

Jie Ding,^a Zhihong Chen,^a Xiaoyin Liu,^a Yuan Tian,^a Ji Jiang,^a Zi Qiao,^a Yusheng Zhang,^a Zhanwen Xiao,^a Dan Wei,^a Jing Sun,^a Fang Luo,^c Liangxue Zhou,^b Hongsong Fan*^a

^a National Engineering Research Center for Biomaterials, College of Biomedical Engineering, Sichuan University, Chengdu 610064, Sichuan, P. R. China

^b Department of Neurosurgery, West China Medical School, West China Hospital, Sichuan University, Chengdu 610064, Sichuan, P. R. China

^c The Center of Gerontology and Geriatrics, West China Hospital, Sichuan University, Chengdu 610064, Sichuan, P. R. China

* Corresponding author: Hongsong Fan (E-mail: hsfan@scu.edu.cn)

29 **Experimental section**

30 Materials: *Bombyx mori* was obtained from Zhejiang Academy of Agricultural Sciences; Multi-
31 walled carbon nanotubes (CNTs) were purchased from Chengdu Organic Chemicals Co. Ltd.,
32 Chinese Academy of Sciences. Nitric acid (HNO_3 , >98%) , paraformaldehyde (>98%), sulfuric
33 (H_2SO_4), *N,N* dimethylformamide (DMF, >99%), ethylene glycol (EG) and hydrogen peroxide
34 (H_2O_2 , >30%) were purchased from Chengdu Kelong Chemical Reagent Factory (China). The BCA
35 Protein Assay Kit was purchased from Beyotime Institute of Biotechnology (Jiangsu, China).
36 Tyramine (TA, >98%) , *N,N*-diisopropylethylamine (DIPEA, >99%), *O*-(7-aza-1*H*-benzotriazol-1-
37 yl)-*N,N,N',N'*-tetramethyluronium hexafluorophosphate (HATU, TCI, >98%), horseradish
38 peroxidase (HRP, 248 U/mg) were purchased from Tokyo Chemical Industry Co., Ltd.; Hyaluronic
39 acid (HA, Bloomage Biotechnology Corporation Limited), sodium periodate (NaIO_4 , Adamas
40 reagent, Ltd.), fluorescein diacetate (FDA), propidium iodide (PI), phalloidin and 4',6-diamidino-2-
41 phenylindole dihydrochloride (DAPI) were purchased from Sigma-Aldrich (USA). 4-aminopyridine
42 (4-AP, 98%) was purchased from Shanghai Acme Biochemical Co., Ltd. All chemicals purchased
43 were of the highest available purity and they were used as received.

44 Preparation of carboxylated CNTs and TA-CNTs: Chemical oxidation of CNTs was carried out
45 using a mixture of sulfuric acid and nitric acid. 0.5 g of CNTs were refluxed with $\text{H}_2\text{SO}_4/\text{HNO}_3$ (3:1)
46 at 70°C for 4 h and diluted three times with ice water, dialyzed at room temperature to neutral
47 and freeze-dried for further use. 50 mg carboxylated CNTs were dispersed in 5 ml DMF and
48 sonicated for 1 h. Next, HATU (0.1141g, 1.5 eq) and DIPEA (100 μl , 3 eq) were added into the above
49 mixture with gently stirring for 15 min. Afterwards, tyramine (0.1372 g, 5 eq) was added into the
50 mixture stirred for 12 h. Finally, tyramine modified CNTs were successfully synthesized after

51 dialysis and freeze-drying.

52 Synthesis of HA-CHO: Firstly, aqueous solution of sodium periodate (0.5 M, 3 mL) was added
53 into HA/aqueous solution (10 mg mL⁻¹, 400 ml) slowly and dropwise, continuously stirring for 4 h
54 in a dark condition at 25 °C. Afterwards, 3 mL EG was added to stop the reaction and magnetically
55 stirred for 1 h, the mixture was collected and dialyzed for 5 days. Finally, the synthesized HA with
56 aldehyde (labeled as HA-CHO) grafted was obtained by lyophilization. The characterization of HA-
57 CHO structure was determined by ¹H-NMR (Fig. S1).

58 Preparation of SF-based hydrogel electrode: Taking the preparation of the Silk/HA-CHO/TA-
59 CNT hydrogel as a typical example. SF based hydrogel electrode were prepared through a facile
60 one-pot *in situ* polymerization. TA-CNT dispersion was sonicated 1h to get uniformly dispersed,
61 and then 8 wt% SF and 8 wt% HA-CHO were mixed with 9:1, 8:2, 7:3 w/v%. Secondly, the desired
62 amount of TA-CNT was mixed into SF/HA-CHO solution. Finally, HRP (500 U/mL) and H₂O₂
63 (0.36~0.37%) were added to crosslink above solutions. SF hydrogels only and with different HA-
64 CHO contents were also prepared, and the detail composition of all types of hydrogels were
65 concluded in Table S1 and S2.

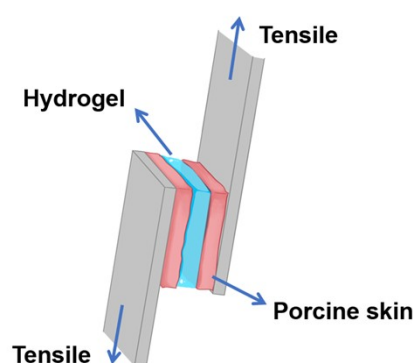
66 Morphology observation: A scanning electron microscope (SEM, S-4800, Hitachi, Japan) was
67 used after hydrogels were freeze dried (accelerating voltage of 5 kV) and hydrogels were sputtered
68 with a conductive gold layer. The morphology of the CNTs with and without modification was
69 observed by transmission electron microscope (TEM, JEOL JEM-2100 F, Japan; acceleration voltage
70 of 200 kV)

71 Mechanical properties: The compression test of the hydrogel electrode was proceeded using
72 dynamic mechanical analysis (amplitude of 20 mm, 5 mN prestress, TA-Q800, US). On the

73 microscopic modulus test, a nanoindentation was carried out using Piuma Chiaro Nanoindenter
74 (Optics 11, Netherland) by putting samples on a glass slide. A spherical cantilever beam ($r=49\ \mu\text{m}$)
75 was used to evaluate the effective Young's modulus (5×5 array, step size= $20\ \mu\text{m}$).

76 Adhesion tests: Tensile adhesion test was performed to investigate the adhesive property of
77 our hydrogels. As shown in Fig. S1, rectangular hydrogel ($10\ \text{mm}\times 10\ \text{mm}$) was sandwiched
78 between the surfaces of two similar porcine skins. Afterwards, the samples (SF, SH and SHC) were
79 pulled by dynamic mechanical analysis instrument at a fixed speed of $1\ \text{mm}\ \text{min}^{-1}$ until separation.

80



81

82 Fig. S1 Schematic illustration of adhesion testing method.

83 Rheology characterization: Rheology measurements were carried out through a rheometer
84 (MCR-302, Anton Paar instrument, Australia). The samples of hydrogels were spread on the round
85 plate. The gelation kinetics of samples were performed via shear oscillation mode (0.5% strain, 10
86 rad/s frequency) at 37°C . Strain sweeps were performed over a strain ranging from 0.1-10% at
87 frequency of 1 Hz and frequency sweeps were performed over a frequency ranging from 0.1-100
88 rad/s at 1% strain at 37°C .

89 Attenuated total reflectance-fourier transform infrared spectroscopy (ATR-FTIR): a Nicolet FTIR
90 6700 spectrometer (Nicolet 6700, Thermal Fisher Scientific Inc., US) was used to check the

91 secondary structure of the hydrogels. The calculation of β -sheet content was performed as the
92 ration of the areas of absorbances at 1616-1621, 1622-1627, 1628-1637 cm^{-1} to total area between
93 1580-1720 cm^{-1} , which was previously reported by Hasturk *et al.*^[1]

94 Electrochemical characterization: The electrochemical workstation Gamry Reference 600
95 potentiostat (Gamry instrument, US) was used for both EIS and CV measurements and connected
96 in the standard three-electrode configuration in 0.1 M PBS solution.

97 To obtain EIS measurements, the hydrogel sheet was sandwiched between two Pt electrodes,
98 and Ag/AgCl was used as reference electrode. The sweep frequency spans from 10 Hz–100 kHz was
99 applied. To measure the charge injection capability, first, hydrogels were synthesized on Pt sheet
100 (1 cm \times 1 cm) as working electrode, a counter electrode (Pt wire, d=0.8 mm) and a reference
101 electrode (Ag/AgCl) were immersed in PBS. Ten successive identical biphasic voltage pulses were
102 applied after stabilization of the system, and the simultaneous current transient was recorded.

103 For the CV measurement, the hydrogels were coated on a platinum sheet with a size of 1 cm^2
104 as a working electrode. A counter electrode (Pt wire, d=0.8 mm) and a reference electrode
105 (Ag/AgCl) were immersed in PBS, finally the curves were obtained from -0.6 V to 0.6V at a scan
106 rate of 100mV/s. The CSC was calculated as following equation:^[2]

107
$$CSC = \int_{t_1}^{t_2} I(t) dt$$

108 Where t_1 is the beginning of CV cycle, t_2 is the end of CV cycle, and I is the current.

109 Epidermal signal recording performance measurement: Before strain or pressure sensing tests,
110 SHC sensor was assembled on the hand or throat of a volunteer. The real-time electrical signals of
111 the strain and pressure sensing based on resistance change of hydrogel electrode were recorded
112 by digital source meter (2612B, Keithley, US). The relative change of the resistance ($\Delta R/R_0$) was

113 calculated by Ohm's law ($R = U/I$) and based on the application of a constant voltage to sensors.
114 The volunteer who participated in the biosignal detection was obtained the informed written
115 consent prior to research, and all the experiments were approved by the Medical Ethics
116 Committee of Sichuan University (KS2022863).

117 *In vitro* biocompatibility of hydrogel electrodes: Cytocompatibility and proliferation was
118 studied by standard MTT measurement and FDA/PI staining. All types of hydrogels were harvested
119 after being co-cultured with BMSCs for 1, 3 and 5 days, and then incubated with MTT (10%) at 37
120 °C for 4 h. Then replacing medium with DSMO and constant temperature oscillation for 15 min,
121 and the absorbance at 490 nm was measured by a multi-detection microplate reader (Bio-Rad
122 550). The morphology of BMSCs was investigated using FDA/PI staining, then imaged with inverted
123 fluorescence microscope (Leica, DMi8 A, German). For cytoskeleton staining, samples were
124 washed fixed in 4% paraformaldehyde solution for 15min and washed 3 times with PBS, then
125 incubated with fluorescein isothiocyanate-labeled phalloidin (5 mg mL^{-1} , 40 min), then stained
126 with DAPI (5 mg mL^{-1} , 5 min) and observed via inverted fluorescence microscope (Leica, DMi8 A,
127 German).

128 Protein adsorption assay: Enhanced BCA Protein Assay Kit was used for measuring the
129 adsorption of BSA on the three types of hydrogels and Pt electrode. The samples were immersed
130 in prepared BSA solutions (0.5 mg mL^{-1}) to incubate at 37 °C for 24h. Then 200 μL BCA work
131 solutions were added into samples solutions to incubate at 37 °C for 20-30 mins. The concentration
132 of BSA was obtained by measuring the absorbance at 562 nm with a microplate reader (BioTek
133 Instruments Inc., US), and then calculated the protein adsorption according to the standard curve
134 and the volume of the sample used.

135 *In vivo* biocompatibility of hydrogel electrodes: All animal experiments were strictly performed
136 with the NIH guidelines for the Care and Use of Research Animals, and approved by the Sichuan
137 Provincial Committee for Experimental Animal Management (approval number: SYXK (Sichuan):
138 2019-189). Sprague Dawley rats (SD rats, Female, 250-300 g, Chengdu Dossy Experimental Animals
139 CO., LTD.) were used and housed for 5-7 days before surgery. Mice were anesthetized using chloral
140 hydrate and shaved, and an 8 mm longitudinal incision was made on the dorsal side with surgical
141 scissors. Sterilized hydrogel and Pt were implanted subcutaneously in SD mice at 2 weeks (n=3).
142 After the end of the 14 days test period, mice were sacrificed and then transcardially perfused
143 with PBS (300 mL) and 4% paraformaldehyde (150 mL). The tissues surrounded with samples and
144 main organs including the heart, liver, spleen, lungs and kidney were excised and collected for
145 histopathological immunological analysis.

146 Histology and immunofluorescence analysis: The inflammatory response of implanted
147 hydrogel and Pt electrode was checked by staining the tissues with H&E (cell cytoplasm
148 (pink)/nuclei (blue)). Then, some slices were immunostained with CD68/DAPI, CD63/DAPI,
149 Collagen I/DAPI and α -SMA for immunofluorescence. All the obtained slices were observed by a
150 multi-spectral automatic scanning system (Vectra 3 S6, Akoya) and analyzed by Inform 2.4.8.

151 *In vivo* epilepsy recording: 4-aminopyridine (2 mg mL^{-1} in PBS solution) was *in situ* injected into
152 the brain of rats. Before that, SD rats were anesthetized with 10% chloral hydrate and the head
153 was fixed on the standard stereotaxic apparatus. After a craniectomy and durotomy, exposing a
154 region of 25 mm^2 on the surface of brain motor cortex for placing hydrogel electrode, and a skull
155 screw wrapped with silver wire was embedded into the left frontal bones as reference. Another
156 Ag wires was connected to an amplifier of a 128-channel neural acquisition processor (Blackrock,

157 USA) and hydrogel electrodes which covered over the exposed cortex for transporting neural
158 oscillation and rhythms. The sampling rate of LFPs was 1 kS/s, with bandpass filtered at 1-250 Hz
159 and the raw neural signals were processed analyzed using a NeuroExplorer software.

160 In epicardial ECG recording: For implantation of hydrogel electrode, SD rats were
161 anaesthetized with 10% chloral hydrate and shaved chest hair. A 37 °C electric heating pad was
162 used for maintaining the body temperature. After thorotomy for exposing living heart, hydrogel
163 electrode was covered on the left atrium as recording electrode, and another needle electrode
164 was used as reference electrode.

165 *In vivo* sciatic nerve stimulation and recording: To perform sciatic nerve bidirectional
166 stimulation and recording, SD rats were anaesthetized with 10% chloral hydrate and shaved the
167 hair. After dissection of the vastus lateralis and biceps femoris to expose the sciatic nerve, hydrogel
168 electrode was adhered on the exposed sciatic nerve. For the electrical stimulation process,
169 biphasic charge-balanced rectangular voltage pulses (0.4-1.2V, 1Hz) were applied by a signal
170 generator and measured the changing angle of the ankle joint with a protractor. For the sciatic
171 recording process, three types of mechanical stimulation including poke, scratch and pinch were
172 applied on the ankle joint of rat, each mechanical stimulus lasted ~10s and was recorded hydrogel
173 electrode connected with neural acquisition processor.

174 Statistically analysis: Statistical analysis was performed with Origin software and Graph Pad
175 7.0. Statistical significance was measured by one or two-way ANOVA test and significance level
176 were set at $p < 0.05$ (*), $p < 0.01$ (**), $p < 0.001$ (***), $p < 0.0001$ (****).

177

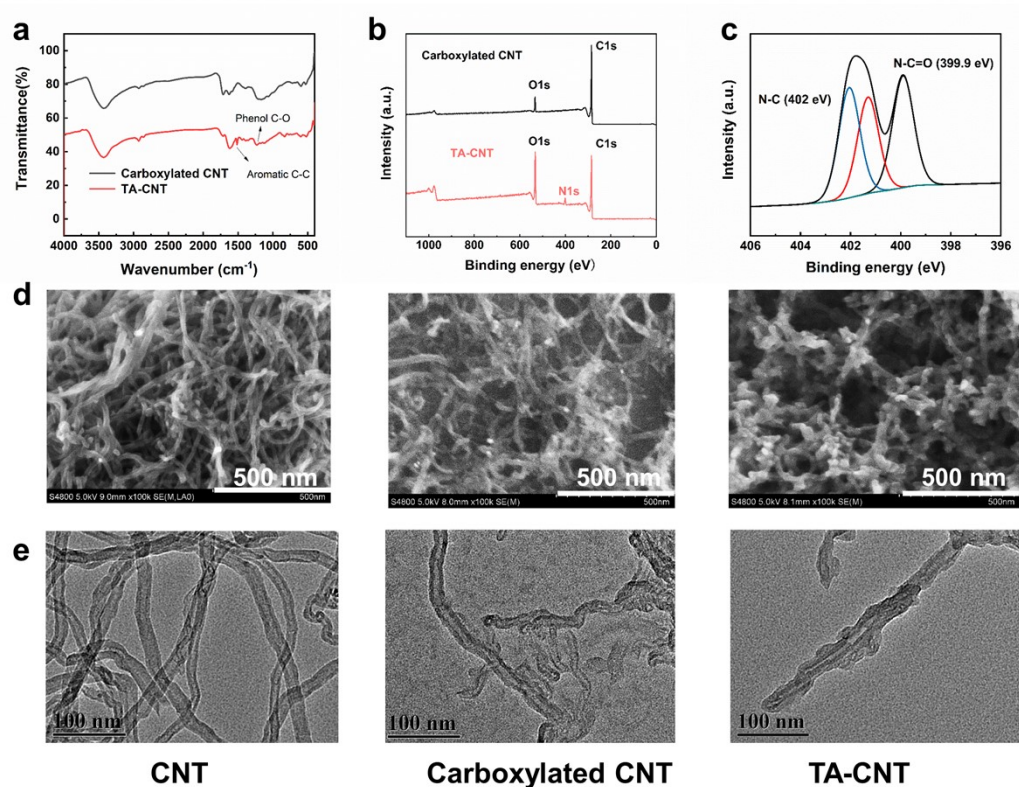
178 [1] O. Hasturk, K. E. Jordan, J. Choi, D. L. Kaplan, Biomaterials, 2020, 232, 119720.

179 [2] K. Krukiewicz, D. Janas, C. Vallejo Giraldo, M. J. P. Biggs, *Electrochim. Acta*, 2019, 295, 253.

180

181

182 **Additional Results**



183

184 Fig. S2. a) FTIR spectrum of prepared carboxylated CNT and TA-CNT. b-c) XPS images of
185 carboxylated CNT and TA-CNT. d) and e) SEM and TEM of CNT, carboxylated CNT and TA-CNT.

186

187

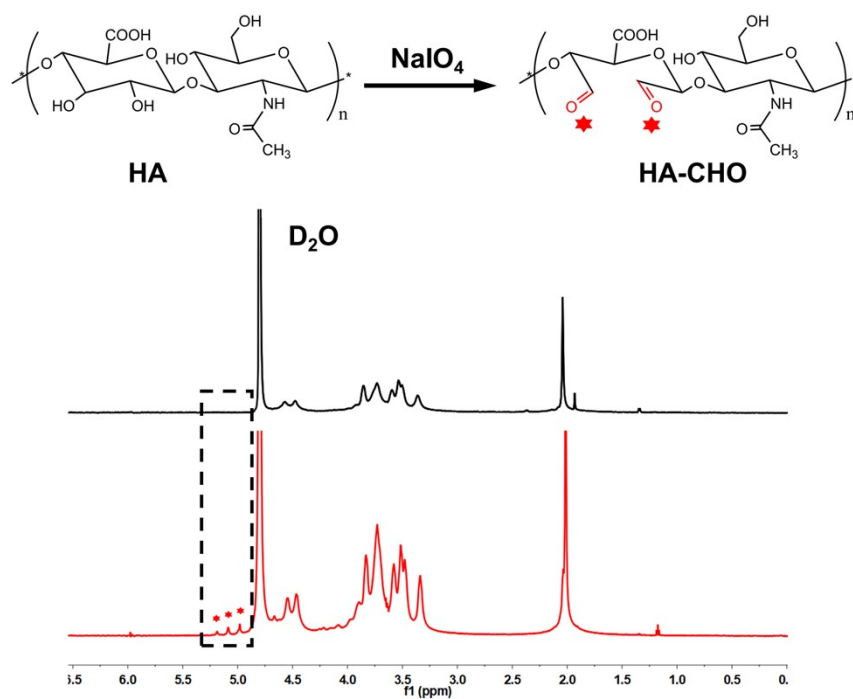
188

189

190

191

192



193

194 Fig. S3. ¹H-NMR spectrum of HA-aldehyde in D₂O. Sodium periodate could oxidize the vicinal diol
195 of HA and generate two aldehyde groups on the HA chains. the chemical shift at 4.97 ppm, 5.09
196 ppm and 5.14 ppm exhibit the presence of aldehyde groups.

197

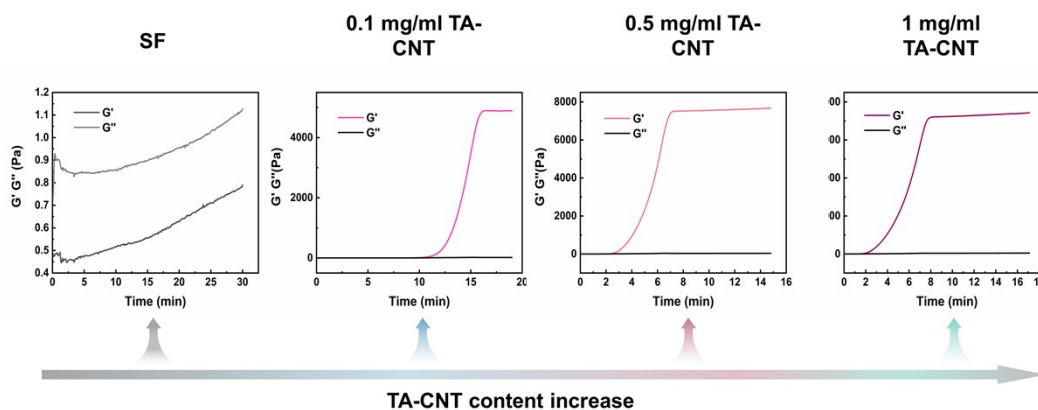
198

199

200

201

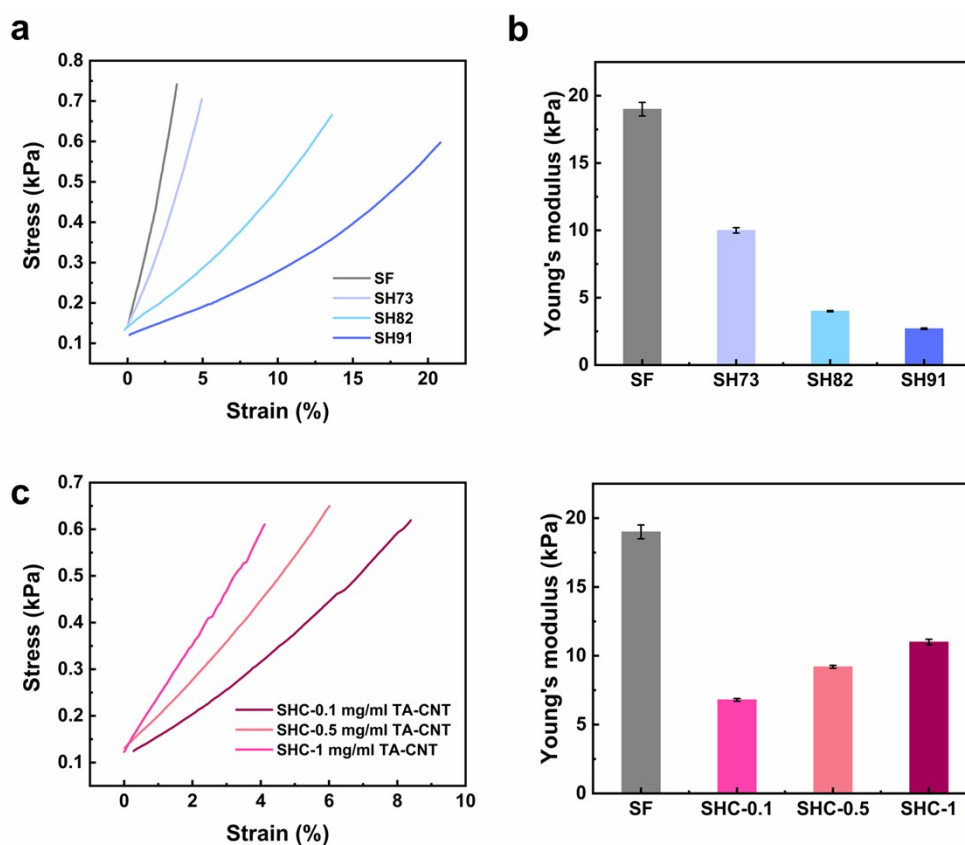
202



203

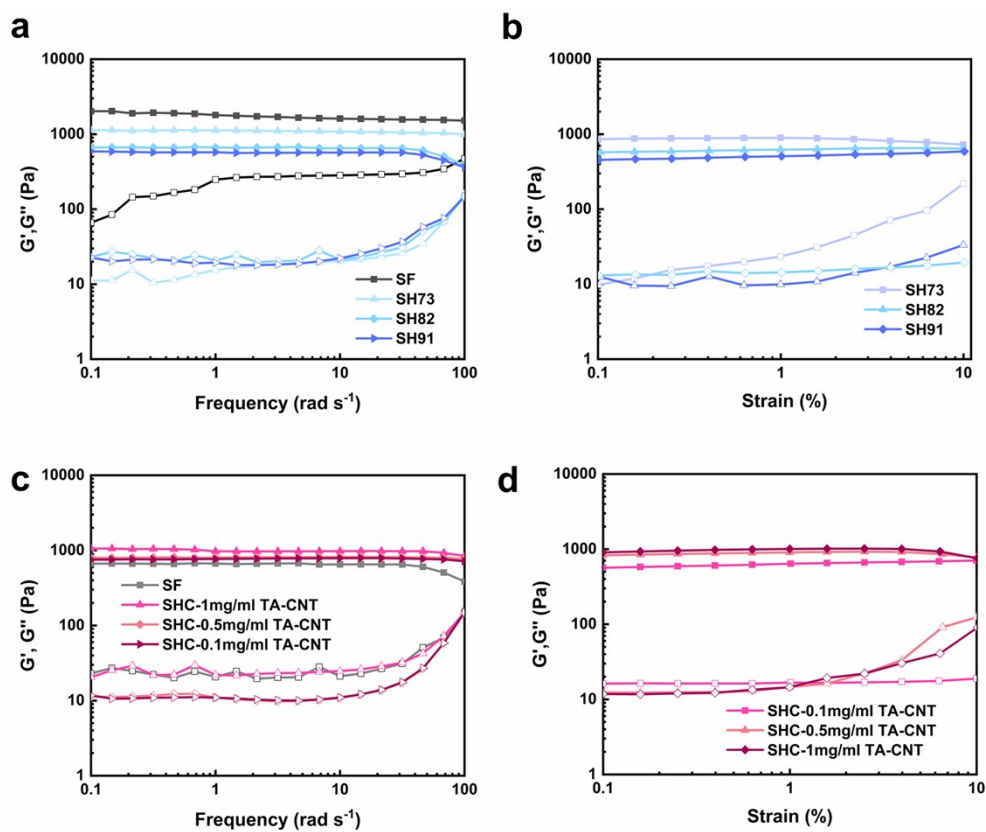
204

Fig. S4. Gel ($G''/G' < 0.05$) points of SHC with increasing contents of TA-CNT.



205

206 Fig. S5. a-b) Compression curves and Young's modulus of SF only and with different HA-CHO
 207 contents, respectively; c-d) Compression curves and Young's modulus of SHC with different TA-
 208 CNT contents, respectively.

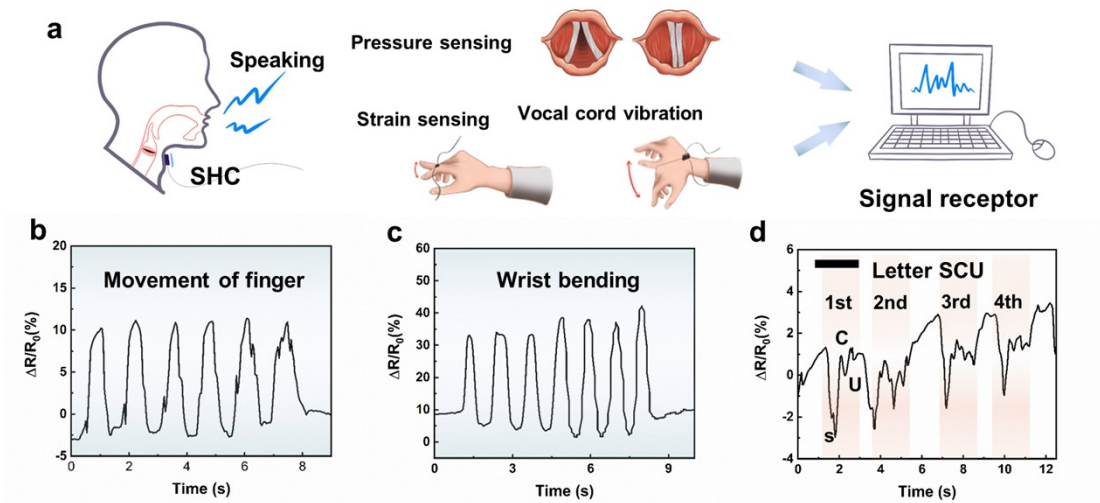


209

210 Fig. S6. (a-b) Frequency sweeps and strain sweeps of SF only and with different contents of HA-
 211 CHO, respectively; (c-d) Frequency sweeps and strain sweeps of SHC hydrogels with different
 212 contents of TA-CNT, respectively.

213

214

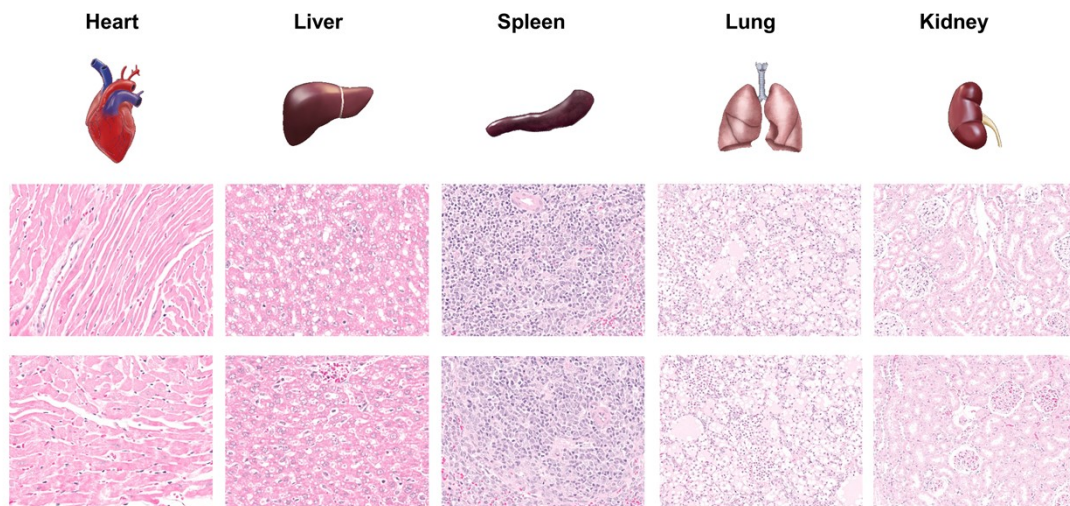


215

216 Fig. S7 a) Schematic illustration of pressure and strain sensing of SHC. b-c) The sensing curves of
 217 finger and wrist movement. d) The curves of sensing speaking in English.

218 As Fig. S7a shown, this potential was initially evaluated by assembling the SHC hydrogel as
 219 surface sensor attached on the skin of a volunteer. Fig. S7b-7c illustrated the resistance changes
 220 with the cyclic bending of the fingers and wrist, which demonstrate epidermal signal recording
 221 properties of the hydrogel electrode. Further, the possibility as pressure sensors for distinguishing
 222 subtle motions such as speaking was proved. By attaching the hydrogel electrode to the neck of a
 223 volunteer, the movement of throat caused by repetitive shocking was clearly recorded by the
 224 resistance change. As Fig. S7d shown, when pronounced specific phrases such as "S" "C" "U", SHC
 225 hydrogel sensor can easily record and distinguish electrical resistance changes caused by vocal
 226 cord vibrations for word recognition.

227



228

229 Fig. S8. Histopathology images of dissected major organs (heart, liver, spleen, lung and kidney)
 230 stained with H&E of control and SHC groups for *in vivo* biosafety evaluation.

231

232

233

Table S1. Composition of the SF-HA-CHO hydrogels

Code	SF (mg mL ⁻¹)	HA-CHO (mg mL ⁻¹)
SF	100	0
SH91	90	10
SH82	80	20
SH73	70	30

234

235

236

237

Table S2. Composition of the SF-HA-CHO/TA-CNT hydrogels

Code	SF (mg mL ⁻¹)	HA-CHO (mg mL ⁻¹)	TA-CNT (mg mL ⁻¹)
SF	10	0	0
SHC-0.1	80	20	0.1
SHC-0.5	80	20	0.5
SHC-1	80	20	1